

Targeted disruption of *Hoxd-10* affects mouse hindlimb development

Ellen M. Carpenter^{1,2,3}, Judy M. Goddard³, Allan P. Davis^{3,*}, T. Paul Nguyen¹ and Mario R. Capecchi^{3,†}

¹Mental Retardation Research Center, UCLA School of Medicine, Los Angeles, CA 90024, USA

²Department of Neurobiology, UCLA School of Medicine, Los Angeles, CA 90024, USA

³Howard Hughes Medical Institute, Department of Human Genetics, University of Utah School of Medicine, Salt Lake City, Utah 84112, USA

*Present address: Oak Ridge National Laboratory, Life Sciences Division, Oak Ridge, TN 37831, USA

†Corresponding author (e-mail: mario.capecchi@genetics.utah.edu)

SUMMARY

Targeted disruption of the *Hoxd-10* gene, a 5' member of the mouse *HoxD* linkage group, produces mice with hindlimb-specific defects in gait and adduction. To determine the underlying causes of this locomotor defect, mutant mice were examined for skeletal, muscular and neural abnormalities. Mutant mice exhibit alterations in the vertebral column and in the bones of the hindlimb. Sacral vertebrae beginning at the level of S2 exhibit homeotic transformations to adopt the morphology of the next most anterior vertebra. In the hindlimb, there is an anterior shift in the position of the patella, an occasional production of an anterior sesamoid bone, and an outward rotation of the lower part of the leg, all of which contribute to the defects in locomotion. No major alterations in

hindlimb musculature were observed, but defects in the nervous system were evident. There was a decrease in the number of spinal segments projecting nerve fibers through the sacral plexus to innervate the musculature of the hindlimb. Deletion of a hindlimb nerve was seen in some animals, and a shift was evident in the position of the lumbar lateral motor column. These observations suggest a role for the *Hoxd-10* gene in establishing regional identity within the spinal cord and imply that patterning of the spinal cord may have intrinsic components and is not completely imposed by the surrounding mesoderm.

Key words: *Hoxd-10*, gene targeting, limb defects, homeosis, neuronal defects, spinal cord defects

INTRODUCTION

The mouse *Hox* complex contains 39 genes distributed in four linkage groups designated *HoxA*, *B*, *C* and *D*. Each gene encodes a transcription factor belonging to the *Antennapedia* homeodomain class. Based on DNA sequence similarities and on the position of the genes on their respective chromosome, individual members of the four linkage groups have been classified into thirteen paralogous families (Scott, 1992). Members of a paralogous family often share common patterns of gene expression and function. Mutational analysis in the mouse has demonstrated that *Hox* genes, alone and in concert with other *Hox* genes, are used to regionalize the embryo along its major axes (reviewed by Krumlauf, 1994). Regionalization of the embryo by *Hox* genes appears to be accomplished by the controlled temporal and spatial activation of these genes, such that a 3' *Hox* gene is activated prior to and in a more anterior region of the embryo than its 5' neighbors (Duboule and Dollé, 1989; Graham et al., 1989; Duboule, 1994). However, *Hox* genes normally function not as individual entities, but as members of highly integrated circuits, such that paralogous genes, adjacent genes on the same linkage groups, and even nonparalogous genes in separate linkage groups interact positively, negatively, and in parallel with each other to orchestrate the morphological regionalization of the embryo (Condie and Capecchi, 1994; Rancourt et al., 1995; Davis et al., 1995; Horan et al., 1995a,b; Davis and Capecchi, 1996; Favier et al., 1996; Fromental-

Ramain et al., 1996a,b; van der Hoeven et al., 1996; Zákány and Duboule, 1996; Chen and Capecchi, 1997).

The sixteen 5' *Hox* genes belonging to the paralogous families 9 through 13 all show DNA sequence similarities to the *Drosophila AbdB* gene, which specifies the identity of the most posterior segments of the larva and adult fly. The homologous mouse genes are also expressed in the posterior region of the mouse embryo and in the developing limbs (Dollé and Duboule, 1989; Dollé et al., 1989). Targeted disruptions of some of these genes have produced defects in the formation of the axial skeleton, in the genesis of posterior internal and external organs, in the specification of motor nerves, and in the patterning of limb bones (Dollé et al., 1993; Small and Potter, 1993; Davis and Capecchi, 1994; Davis et al., 1995; Satokata et al., 1995; Rijli et al., 1995; Davis and Capecchi, 1996; Favier et al., 1996; Fromental-Ramain et al., 1996a, b; Kondo et al., 1996; van der Hoeven et al., 1996; Zákány and Duboule, 1996). In this paper we describe the defects associated with the disruption of *Hoxd-10*. The 10th paralogous gene family contains three members, *Hoxa-10*, *Hoxc-10* and *Hoxd-10*. The consequences of mutating the *Hoxc-10* gene have not been reported, but description of an ES cell line with a mutation in the *Hoxd-10* gene has been published (Rijli et al., 1994). However, generation of ES cells with this mutant allele appears to have compromised the ES cell line, since mouse chimeras made from this cell line die in utero. Mice homozygous for the *Hoxa-10* mutation show anterior homeotic transformations of the lumbar

vertebrae, male and female sterility, anterior transformations of thoracic and lumbar motor neurons, and defects in the proximal hindlimbs (Rijli et al., 1995; Satokata et al., 1995; Favier et al., 1996). Except for the defects in the hindlimbs, there is remarkably little overlap between the reported mutant phenotypes resulting from disruption of *Hoxa-10* and those we describe here resulting from *Hoxd-10* disruption. In *Hoxd-10* mutants, anterior transformations of the axial skeleton are restricted to the sacral and first caudal vertebrae. Similarly, the neuronal defects seen in *Hoxd-10* mutant homozygotes are posterior to those observed in *Hoxa-10* mutants.

MATERIALS AND METHODS

Generation of *Hoxd-10* mutant mice and genotype analysis

A replacement-type gene targeting vector composed of 14.8 kilobases (kb) of genomic DNA containing the *Hoxd-10* gene and flanked by two *thymidine kinase* genes was constructed in a pUC plasmid (Fig. 1; Thomas and Capecchi, 1987; Deng et al., 1993). To disrupt the *Hoxd-10* gene, the *neomycin resistance (neo^r)* expression cassette KT3NP4 (Deng et al., 1993) was inserted at the *HpaI* site in exon 2 in the same transcriptional orientation as the *Hoxd-10* gene. The cleavage site corresponds to amino acid 38 in the second alpha-helix of the homeodomain.

The targeting vector was linearized and electroporated into R1 ES cells (Nagy et al., 1993), and cell selection and DNA extraction were performed as described by Mansour et al. (1988); Davis and Capecchi (1994). A primary screen for the cell lines containing targeted disruption of the *Hoxd-10* locus was done by Southern blot analysis of *SphI*-digested genomic DNA using a 2.6 kb *XhoI/SphI* 3' flanking probe (3' f.p., Fig. 1). This probe hybridizes to a large fragment (greater than 23 kb) in wild-type DNA and to a 12.1 kb DNA fragment in the *Hoxd-10* mutant allele. Additional diagnostic digests and probe hybridizations (including a *neo*-specific probe) confirmed the integrity of the targeting event (data not shown). One out of 123 cell lines analyzed tested positive for a gene targeting event. This ES cell line was injected into C57Bl/6J (B6) blastocysts to produce chimeric males that transmitted the mutation through the germline.

For genotyping, DNA was isolated from tail biopsies or yolk sacs and analyzed by Southern blotting, as described above, or by gel electrophoresis of PCR-amplified DNA. The primers used for the PCR reaction were: *Hoxd-10* sense primer, 5'CCCTTACACCAAGCACCAAACG (nucleotides 2543-2564; Renucci et al., 1992); *Hoxd-10* antisense primer, 5'CTCGGATCCTGGCCTCACATC (nucleotides 2765-2785); KT3NP4 antisense primer, 5'TTCAAGCCCAAGC-TTTCGCGAG (junction of RNA polymerase II and the pIC19R polylinker; Deng et al., 1993). The sizes of the wild-type and *Hoxd-10* mutant bands are 242 base pairs (bp) and 130 bp, respectively.

Carbocyanine dye tracing

Embryos were collected at E12.5, pinned and fixed as described by Carpenter et al. (1993). To label spinal nerves in the sacral plexus, dye injections were made using a 0.5% solution of DiI (Molecular Probes) in dimethylformamide. Dye was injected at the base of the hindlimb bud using multiple short pulses generated by a Picospritzer (General Valve). Dye transport was allowed to proceed at room temperature in the dark for 48 hours. Embryos were then eviscerated and dissected to expose the spinal cord and nerves entering the hindlimbs. Animals were initially examined using a Leitz Ortholux microscope equipped with a rhodamine filter set. Further observations were made with a BioRad MRC-600 confocal microscope. Images were collected as a Z-series at 1 µm intervals and merged to a single frame for further analysis.

Histology and skeletal preparations

Newborn mice were fixed in Bouin's solution at room temperature for 1 week, dehydrated through graded ethanol and xylene and embedded in paraffin. 10 µm serial sections were collected and stained with hematoxylin and eosin (Chisaka and Capecchi, 1991). Age and sex-matched littermates were collected and used for skeleton preparations as described (Mansour et al., 1993).

Whole-mount immunohistochemistry

Embryos were pinned and fixed (Carpenter et al., 1993) and then eviscerated to expose the ventral side of the spinal column and the nerves and plexus at the base of the hindlimb. Embryos were refixed in 4:1 methanol (MeOH):dimethylsulfoxide (DMSO) overnight at room temperature, bleached with 6% H₂O₂ in 4:1 MeOH:DMSO, and rehydrated through graded MeOH:PBS with addition of 0.5% Tween 20 (PBST) to 100% PBST. Embryos were blocked with PBST, 2% skim milk powder, 1% DMSO, and then incubated overnight at 4°C in a 1:1 dilution (in blocking solution) of the 2H3 antibody (Developmental Studies Hybridoma Bank) directed against a subunit of the neurofilament protein. Horseradish peroxidase-conjugated goat anti-mouse secondary antibody (Jackson Immunoresearch) was used at a dilution of 1:100 and detected with 0.0015% H₂O₂ in 1 mg/ml diaminobenzidine (DAB)/PBST. Embryos were rinsed, then stained overnight with 0.02% alcian blue 8GX as described by Rancourt et al. (1995). The skin was gently peeled away from the hindlimbs and the embryos photographed under a dissecting microscope.

Whole-mount in situ hybridization

Embryos were collected at E12.5 and E13.5, fixed overnight in 4% paraformaldehyde/PBS and processed for whole-mount in situ hybridization with *Hoxd-9* and *Hoxd-11* antisense RNA probes as previously described (Carpenter et al., 1993). The *Hoxd-9* probe was made from a 770 bp *PstI-EcoRI* fragment in the 3' untranslated region of the *Hoxd-9* gene (Renucci et al., 1992); the *Hoxd-11* probe was made from a 300 bp *AccI-BamHI* fragment from the *Hoxd-11* gene including part of the homeodomain and 3' untranslated sequence (Duboule, 1991). Probes were labeled with digoxigenin-11-UTP (Boehringer Mannheim) and detected with alkaline phosphatase-conjugated antibodies directed against digoxigenin (Boehringer Mannheim). Alkaline phosphatase reaction product was visualized with NBT and BCIP (Boehringer Mannheim).

RESULTS

Targeted mutagenesis of *Hoxd-10*

A targeting vector designed to disrupt the *Hoxd-10* locus (Fig. 1) was electroporated into R1 ES cells. One cell line, shown by Southern blot analysis to carry the *Hoxd-10* mutant allele, was used to generate chimeric mice that transmitted the mutant allele through the germline (see Materials and Methods). Genotypes at birth and at weaning segregated in the expected Mendelian ratios showing no preferential loss of mutant homozygotes.

Alterations in gait, adduction, and male fertility

Adult *Hoxd-10* mutant mice exhibited hindlimb defects manifested in two locomotor phenotypes: an abnormal gait and adduction, the inability to bring their hindlegs towards the ventral midline. The gait phenotype varied in severity, with 24% of the mice acting outwardly normal; the remainder demonstrated mild to severe deficits (Table 1). In mildly affected mice, the gait was jerky, with the hindlimbs being stiff, but not spastic; the hindfeet were splayed out in an abnormal

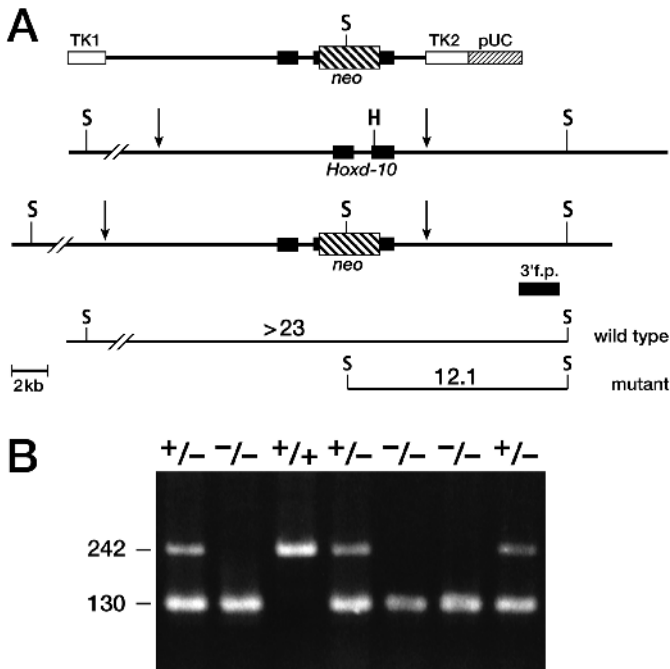


Fig. 1. Targeted mutagenesis of *Hoxd-10* and genotype analysis of mice. (A) The diagram illustrates the targeting vector (upper line) and the anticipated restriction fragment lengths (lower two lines) resulting from a gene targeting event. *Hoxd-10* exons 1 and 2 are depicted by black boxes; the *neo* cassette disrupts the second exon at the *HpaI* site; the white boxes are the *thymidine kinase* genes TK1 and TK2, and the plasmid vector backbone is marked as pUC. The vertical arrows represent the ends of the genomic DNA used to construct the targeting vector. *SphI* digests, when hybridized with a 3' flanking probe (3' f.p.) showed a mutant band of 12.1 kb, downshifted from the wild-type band of >23 kb (data not shown). H, *HpaI*; S, *SphI*. (B) Example of PCR/electrophoretic gel analysis of genotypes resulting from a *Hoxd-10* heterozygous intercross. DNA bands amplified from the wild-type and mutant alleles are 242 and 130 bp, respectively.

posture. Severely affected mice had very stiff hindlimbs, walked with their hindlimbs outstretched behind them, and swung their hindfeet forward with effort in order to support their weight. In some cases, the animal put its weight on the top of the foot rather than the bottom. Affected hindlimbs retracted in response to touch. One heterozygous animal also had a mild gait defect, but others were unaffected. These defects were present in mutants as they first began to walk and were not progressive.

To test adduction, a mouse was positioned on a pencil along its ventral midline (Fig. 2). When support was withdrawn, wild-type and heterozygous *Hoxd-10* mice responded by gripping the pencil with both of their forefeet and hindfeet and were able to maintain balance (Fig. 2A). Mutant homozygotes were unable to grip the pencil with their forepaws, but were able to bring their hindfeet together to grip the pencil (Fig. 2B). Most mutant animals tested showed this adduction deficit, even those in which the gait defects were minimal (Table 1). A single heterozygous animal was also unable to grip the pencil.

An additional defect apparent in adults was a marked decrease in fertility in mutant homozygous males. Six mutant

Table 1. Number of *Hoxd-10* mutant mice with defects in gait and adduction

Genotype	No gait defect	Mild gait defect*	Severe gait defect†	Adduction defect
+/+	5/5	0/5	0/5	0/5
+/-	10/11	1/11	0/11	1/11
-/-	7/29	17/29	5/29	25/29

*Mild gait defects: jerky gait, slight hindlimb stiffness, abnormal foot posture.
 †Severe gait defects: pronounced hindlimb stiffness, abnormal posterior hindlimb extension, improper weight distribution on dorsal surface of foot.

males were tested in three trials for their ability either to mate (as judged by the presence of copulation plugs) or to induce a pregnancy. One of these six males impregnated a female on one mating trial; all other males were unable to copulate. Histological sections through the male reproductive system revealed no differences relative to control animals (data not shown). The testes had descended, all of the reproductive organs appeared normal, and normal quantities of sperm were present in the epididymis and vas deferens. The decreased fertility may be due to the hindlimb locomotor problems interfering with mounting.

Six homozygous mutant female mice were tested for fertility in matings with heterozygous or wild-type males. All females were able to produce offspring, but there was significant mortality in the first two litters from four of these females. All pups died during the first postnatal day with an absence of milk in their stomachs. Pups taken from such crosses and fostered with lactating Swiss Webster females survived to adulthood. However, in subsequent litters, these mutant females were able to successfully raise their pups.

Alterations in the axial and appendicular skeleton

Mice normally possess four sacral vertebrae. The most anterior sacral vertebra (S1) fuses with the pelvis to anchor the pelvic girdle. Both S1 and S2 vertebrae have winged transverse processes, while S3 and S4 have anteriorly projecting, club-shaped processes. In wild-type animals, S1, S2, and S3 are fused with each other at the tips of their transverse processes, while S4 remains unfused (Fig. 3A). Fifteen mutant skeletons were examined for changes in the sacral and caudal vertebrae. Mutant animals showed an increased number of fused sacral vertebrae and alterations in the shape of the transverse processes (Fig. 3B,C). Most had three or four sacral vertebrae with winged transverse processes compared with only two seen in wild-type animals. Half of the mutant animals also had four and occasionally five fused vertebrae (Fig. 3). Two heterozygous animals also had unilateral fusions of four transverse processes. Additionally, in mutants, both the S1 and S2 vertebrae articulated with the pelvis. This is suggestive of an anterior transformation of the S2 vertebra into an additional S1 with more posterior sacral and anterior caudal vertebrae assuming a more anterior phenotype.

Skeletal alterations were also observed in the hindlimbs of mutant animals. The position of the patella was shifted upward to the forward surface of the femur in 13 of 16 mutant hindlimbs examined (Fig. 4A-D). In addition, an ectopic sesamoid bone was observed embedded in the patellar tendon at the proximal edge of the patella in 5 of 16 mutant animals

Fig. 2. Hindlimb adduction in wild-type (A) and *Hoxd-10* mutant (B) mice. Wild-type animals can grip a pencil with both forelimbs and hindlimbs, while mutant mice are unable to bring their hindlimbs together in order to grip the pencil with their hindfeet (arrow).

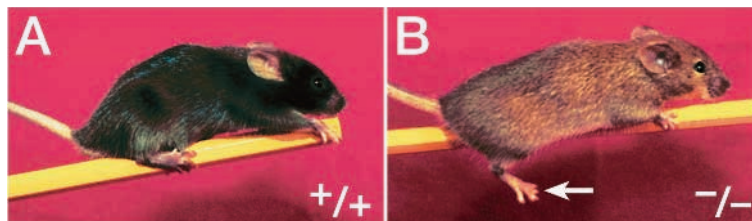


(Fig. 4D). Based on similarities in shape and position to the lateral sesamoid bones, this bone was termed an anterior sesamoid. Ectopic sesamoids are often generated as a secondary remodeling response to changes in tension at a joint (e.g., Davis and Capecchi, 1994; Favier et al., 1996).

Changes were also noted in the articulation between femur and tibia which were shifted out of alignment with the tibia rotated outward (Fig. 4E,F). Rotations were observed in 10 of 16 mutant hindlimbs. These rotations result in an abnormally positioned foot.

Alterations in the nervous system

We examined the developing nervous system by carbocyanine dye tracing, immunohistochemistry and histological analysis. Dye tracing was used to examine limb innervation in five wild-type and seven mutant animals during development. Injections of the lipophilic tracer DiI were made into the base of the developing limbs at E12.5. DiI retrogradely labeled spinal motor neuron somata (Fig. 5A,B) and anterogradely labeled the distal projections of these neurons through the lumbosacral plexus into the limb (Fig. 5C-F). In humans and mice, the lumbosacral plexus has two components: the rostral lumbar plexus and the caudal sacral plexus. Due to the positioning of the embryos during the injections and the position of the plexus elements within the developing hindlimb at E12.5, the DiI injections primarily labeled motor neurons whose fibers pass through the sacral plexus. These fibers travel along the posterior margin of the femur and diverge to form the major

nerve trunks providing distal limb innervation. The major nerve arising from this plexus is the sciatic nerve, which branches at the level of the knee to form the tibial and peroneal nerves that innervate the musculature of the lower leg and foot (Marieb, 1995). In nine out of ten limbs examined in five control animals these injections intensely labeled four spinal nerves. The two central nerves contained the largest complement of labeled fibers. These four nerves emerge from lumbar segment L3 through L6. In a single control embryo, fibers emerging from only three spinal segments were observed on one side of the animal. Fibers from all labeled nerves coalesced to pass through the pelvic girdle and the sacral plexus, then diverged into multiple branches in the limb.

Seven mutant embryos were analyzed by carbocyanine dye tracing. One of these embryos had four labeled spinal nerves providing sacral plexus fibers on both sides of the animal. Four animals had four spinal segments providing motor innervation on one side and three spinal segments on the contralateral side (Fig. 5B). The remaining two animals had three segments providing motor innervation bilaterally. In mutant animals having four labeled spinal nerves, the contributions of the most anterior and posterior segments were reduced compared with

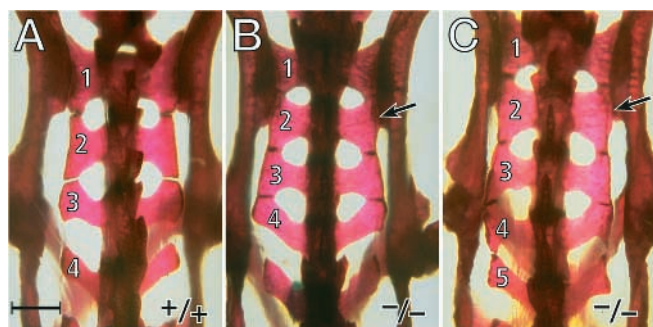


Fig. 3. Sacral vertebrae in wild-type and *Hoxd-10* mutant adult mouse skeletons. (A) Wild-type animals have two sacral vertebrae with wing-shaped transverse processes (S1, S2), a transitional third sacral vertebra (S3), and one unfused fourth sacral vertebra (S4). (B) In mutants, the first three sacral vertebrae and sometimes the fourth (C) all have wing-shaped transverse processes. In wild-type animals, the first three sacral vertebrae are fused, while in mutants the fourth and sometimes fifth sacral vertebrae are fused. In wild-type animals, only the first sacral vertebra articulates with the ilium, while in mutants, the second sacral vertebra articulates as well (arrows in B and C). Scale bar, 2 mm.

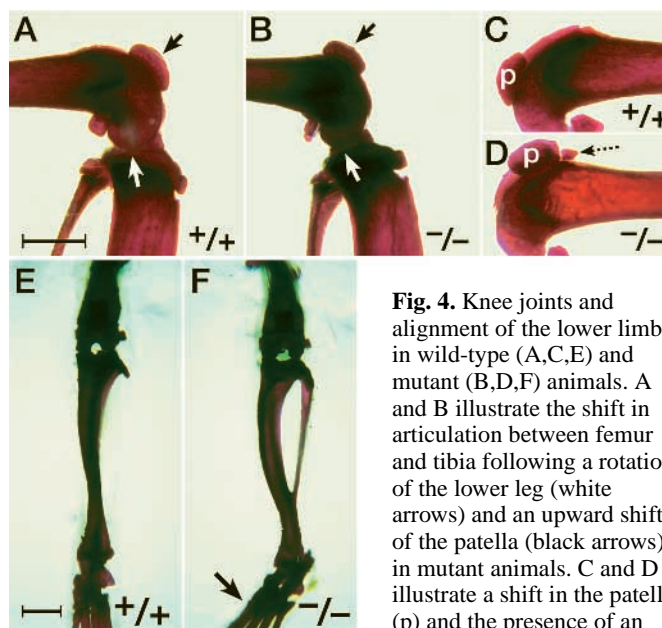


Fig. 4. Knee joints and alignment of the lower limb in wild-type (A,C,E) and mutant (B,D,F) animals. A and B illustrate the shift in articulation between femur and tibia following a rotation of the lower leg (white arrows) and an upward shift of the patella (black arrows) in mutant animals. C and D illustrate a shift in the patella (p) and the presence of an additional bone, the anterior sesamoid, anterior to the

patella (dotted arrow in D) in mutant animals. E and F show a frontal view of the right knee joint and lower limb in wild-type (E) and *Hoxd-10* mutant (F) mice. In F, the tibia has rotated off axis resulting in a lateral twisting of the foot (arrow). The underlying fibula is now exposed. Scale bar, 2 mm.

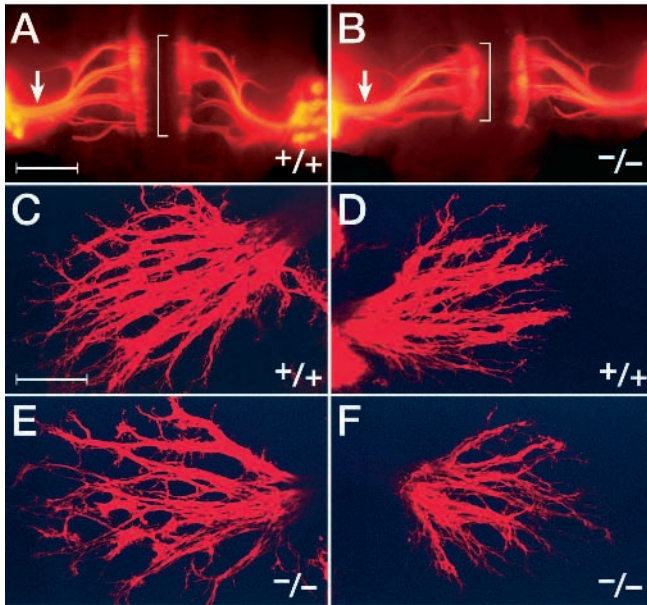


Fig. 5. Carbocyanine dye fills of motor nerves and distal nerve arbors in wild-type (A,C,D) and *Hoxd-10* mutant (B,E,F) mice at E12.5. In wild-type embryos, four spinal nerves are labeled following dye injection at the base of the hindlimb (injection sites visible at lateral margins of the field in A). In the mutant embryo (B), four spinal nerves are labeled on one side and three on the other. In the mutant embryos having four spinal nerves labeled, the labeling in the most anterior and most posterior nerve is greatly reduced. The labeled nerves join together at the posterior margin of the limb to form the sacral plexus (A, B arrows). Retrogradely labeled motor neuron somata in the spinal cord (A,B, brackets) are also visible; note the reduction of this domain in the mutant embryo (B). C, D, E, and F illustrate the distal arbors of the tibial nerve in right hindlimbs (C,E) and left hindlimbs (D,F) of wild-type (C,D) and mutant (E,F) animals. The number of nerve fibers and the branching density is substantially reduced in the mutant animals. Scale bar for A and B, 800 μm , and for C, D, E, and F, 100 μm .

the contributions from the same segments in control animals. In animals with only three labeled segments, the most anterior segment was missing.

Anterograde tracing with DiI also showed alterations in terminal nerve arborizations of the tibial nerve in mutant animals (Fig. 5C-F). This nerve was tipped with a flattened, hand-shaped terminal arbor of axons, which were bundled into many large fascicles with smaller branching fascicles growing toward their targets. Terminal arbors of this nerve in mutant animals showed a decrease in the size and density of the fascicles (Fig. 5C-F). Labeling of E12.5 embryos with the 2H3 neurofilament antibody showed a similar reduction in the density of these terminal arbors (data not shown).

To visualize the complete set of nerves as it innervates the developing hindlimb, animals at E13.5 were examined using whole-mount labeling with the 2H3 antibody (Fig. 6). As the spinal nerves enter the developing hindlimb, they diverge into the lumbar and sacral plexuses which are positioned respectively anteriorly and posteriorly around the head of the femur. Muscle nerves branch off distally from these plexuses to provide the innervation to the hindlimb musculature. In 3 of 10 mutant hindlimbs examined, one of these muscle nerves, the

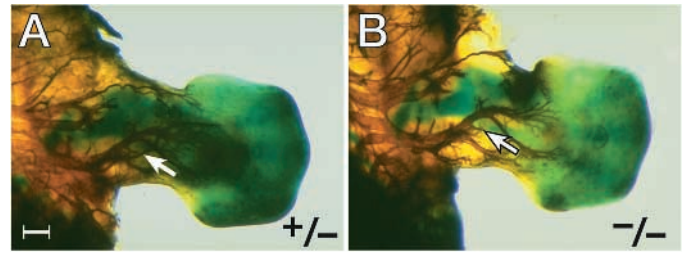


Fig. 6. Antineurofilament stained nerves in hindlimbs of *Hoxd-10* mutant heterozygous (A) and homozygous (B) E13.5 embryonic mice. The peroneal nerve is present in the control animal but absent in the mutant (arrows). Scale bar, 200 μm .

peroneal nerve, was missing (Fig. 6). This nerve was present in all 21 heterozygotes and 6 wild-type control hindlimbs examined.

Transverse sections of newborn animals showed that the spinal cord, dorsal root ganglia, and spinal nerves were grossly normal in mutant animals (Fig. 7). Spinal nerves emerged from the appropriate intervertebral level accompanied by Schwann cells and followed normal trajectories to innervate the limb. Dorsal root ganglia were located in the expected places and appeared normal in size and shape. The spinal cord appeared to be the same size as in littermate controls, and its laminar organization appeared normal. The carbocyanine dye injections suggested that there might be some alterations in the population of motor neurons innervating the hindlimb, so the morphology and position of spinal motor neurons and the lateral motor column (LMC) were examined. The LMC containing the motor neurons that provide hindlimb innervation is present in the spinal cord in five lumbar segments, L1 through L5 in newborn mice (Lance-Jones, 1982). Motor neurons residing in this column can be identified by size and position, and partial identification of the target of innervation of particular groups of motor neurons may be made based on their relative position within the LMC (McHanwell and Biscoe, 1981). A population of large, ventrolaterally positioned cells resembling spinal motor neurons was readily visible in transverse sections through wild-type and mutant newborn animals (Fig. 7). In our wild-type animals, however, these cells extended more rostrally than reported, beginning opposite the rostral portion of thoracic (T) vertebra 13 and continuing posteriorly into L5. The majority of LMC motor neurons were adjacent to the L1 and L2 vertebrae, with smaller populations present as far caudally as L5. This change in position may reflect differences between the mouse strain used for previous motor neuron mapping studies (CD1) and the strains used in construction of *Hoxd-10* mutant mice (B6 and 129). In mutant animals, the LMC neurons were displaced posteriorly by half a segment, with the neurons first appearing near the middle of the T13 vertebra. The largest populations of these neurons were adjacent to the L2 and L3 vertebrae.

Gross anatomy of hindlimb musculature and innervation

Hindlimbs from six mutant and four wild-type adult animals were examined for alterations in the organization of musculature. Muscles from the anterior, medial and lateral compartments of the distal part of the leg were dissected and scored

for the presence and the appearance of the musculature (Table 2). Mice have five muscles in the lateral compartment, in contrast to humans which have only three muscles in comparable locations (Marieb, 1995). Three of these five muscles, peroneus brevis, peroneus longus, and peroneus tertius, were correlated with their human counterparts. Two additional muscles provide fine motor control of the fourth and fifth digits. We have termed these additional muscles the fourth digit dorsolateral and the fifth digit lateral, based on the position of their tendon insertion sites into the fourth and fifth digits. In general, the musculature of the mutant animals appeared grossly normal. Most muscles were present in their expected locations; the only differences noted with some frequency were the misrouting of tendons to their insertion points (Table 2). This may be a response to alterations in the position of the leg imparted by the skeletal abnormalities described above. Cross sectional area and muscle position were also examined on sections taken through hindlimbs of newborn animals. Muscles and their positions in mutant animals appeared normal in comparison to wild-type littermates (data not shown).

Muscle nerves were also examined in dissected hindlimbs and the presence and position of six nerves were scored (Table 2). With the exception of a slight reduction in the size of the common peroneus in two mutant animals, there were no differences in the position and trajectory of the hindlimb nerves examined.

***Hoxd-9* and *Hoxd-11* expression appears normal in *Hoxd-10* mutant homozygotes**

The expression of *Hoxd-9* and *Hoxd-11* was examined in *Hoxd-10* mutant embryos (E12.5 to E13.5) to determine

Table 2. Number of *Hoxd-10* mutant mice examined for hindlimb muscles and nerves

	Genotype	
	+/+	-/-
Muscles		
Anterior		
Extensor digitorum longus	8/8	12*/12
Tibialis anterior	8/8	12‡/12
Extensor hallucis longus	8/8	10/12
Medial		
Flexor digitorum longus	8/8	12/12
Tibialis posterior	8/8	12‡/12
Flexor hallucis longus	2/6	7/10
Lateral		
Peroneus brevis	8/8	12§/12
Peroneus longus	8/8	12/12
Peroneus tertius	5¶/5	9**/10
4th digit dorsolateral	5/5	8/8
5th digit lateral	4/4	7††/8
Nerves		
Femoral	8/8	12/12
Saphenous	8/8	12/12
Sciatic	8/8	12/12
Common peroneus	6/6	10‡‡/10
Tibialis	6/6	10/10
Posterior femoral cutaneous	6/6	10/10

*1 abnormal (shifted laterally); †2 abnormal (reduced or shifted); ‡1 abnormal (tendon displaced); §1 abnormal (duplicated tendon); ¶1 abnormal (bifurcated tendon); **1 reduced, 1 potentially absent (or 5th digit lateral); ††1 missing (on p. tertius); ‡‡ reduced in 2 cases.

whether the disruption of *Hoxd-10* affected the expression patterns of neighboring genes. Expression of *Hoxd-9* in wild-type, *Hoxd-10* heterozygous, and *Hoxd-10* homozygous mutant embryos was found in forelimb, hindlimb, spinal cord, and prevertebrae adjacent to the hindlimbs as previously reported (Dollé and Duboule, 1989). In wild-type embryos at E12.5, *Hoxd-9* expression had an approximate anterior border in the spinal cord at the level of prevertebra 19. High levels of expression were maintained posteriorly through anterior lumbar segments and then decreased at more caudal levels. Labeling in the prevertebrae was observed beginning at prevertebra 22 and continued caudally for approximately 8 segments. The patterns of *Hoxd-9* expression were not altered in *Hoxd-10* heterozygous and mutant homozygous embryos (data not shown). Like *Hoxd-9*, *Hoxd-11* is normally expressed in the spinal cord, prevertebrae and developing limb buds (Izpisua-Belmonte et al., 1991). The patterns of *Hoxd-11* expression in wild-type, *Hoxd-10* heterozygous and *Hoxd-10* homozygous embryos were indistinguishable (data not shown).

DISCUSSION

Targeted disruption of the *Hoxd-10* gene results in mice with adduction and gait defects affecting the hindlimbs. In these mutants, both the axial and appendicular skeletons are affected, as is the organization and robustness of the hindlimb motor innervations. These alterations may provide a cause for the observed defects in locomotion and reproductive behavior.

Disruption of the *Hoxd-10* gene results in anterior transformation of sacral vertebrae, with S2 transformed into a second S1 and three to four more posterior vertebrae also adopting a more anterior morphology. This results in a duplication of S1 and a secondary articulation to the ilium. Disruption of the paralogous gene *Hoxa-10* also results in homeosis, though at a more anterior level, with L1 transformed into T14 and L2, L3 and L4 acquiring characteristics normally associated with their immediate anterior vertebrae, respectively (Rijli et al., 1995). Curiously, disruption of the more 5' *Hox* gene, *Hoxd-11*, also results in a slightly more anterior homeotic transformation in the lumbosacral region, with S1 being transformed to a 7th lumbar vertebra, S2 to S1 and so on (Davis and Capecchi, 1994; Favier et al., 1995). In this context the transformations resulting from the *Hoxd-10* mutation appear to be more posterior than anticipated either from the behavior of mutations in paralogous family members and adjacent 5' genes, or from the anterior limit of *Hoxd-10* expression in the prevertebrae. Clearly it is the coordinated temporal and spatial expression of multiple *Hox* genes in any given region that specifies the identity of groups of vertebrae. Disruption of any given *Hox* gene results in a break in this coordinated pattern. The mutant phenotype is exposed in the region of minimal functional overlap. Often this occurs at the anterior limit of expression of the mutant gene; however, in the case of *Hoxd-10*, it occurs at a more posterior level. It is important to remember, however, that the expression patterns of these genes are dynamic and that the quantitative output, i.e., how many *Hox* genes are expressed in a given region, is as important as which specific *Hox* genes are expressed in the region. Thus, the point of minimal functional overlap could occur early or late during the formation of the affected vertebrae.

Skeletal alterations are also observed in the hindlimbs of *Hoxd-10* mutants, including a shift in the position of the patella, and the presence of an ectopic sesamoid. These changes are likely to involve the patellar tendon, in which both the patella and the anterior sesamoid are embedded. Altering the tension produced by this tendon through shortening and/or improper alignment might cause the anterior shift of the patella with a simultaneous shift forward of the lower part of the hindlimb skeleton, affecting the articulation between femur and tibia. This would destabilize the knee joint and produce the outward rotation in the lower part of the leg. There were no alterations in the shape of the distal part of the femur and no extra ligaments that might provide an alternate explanation for the reshaping and destabilization of the knee joint, as is observed in the *Hoxa-10* mutant hindlimbs (Favier et al., 1996). The defects in the formation of the knee are consistent with strong expression of *Hoxd-10* in this joint (Dollé and Duboule, 1989; Favier et al., 1996). The destabilization of the knee joint and rotation of the lower limb could be sufficient to explain the defects in gait and adduction.

Unexpectedly, mutations in *Hoxa-10*, *Hoxd-10* and even in *Hoxc-10* (S.L. Hostikka and M. Capecchi, unpublished results) primarily cause defects in the formation of the knee joint. Mutations in other 5' *Hox* genes primarily affect the formation of forelimbs (*Hoxa-11*, *Hoxd-11* and *Hoxd-12*) or both fore- and hindlimbs (*Hoxa-13* and *Hoxd-13*). However, the elbow and knee joints are particularly disparate structures and their differences need to be genetically programmed. It appears that one of the roles of *Hox-10* paralogs is to mediate the formation of these structural and functional differences.

Disruption of *Hoxa-10* affects male fertility due to a malformation in the gubernaculum (Rijli et al., 1995; Satokata et al., 1995). Though male fertility was affected in *Hoxd-10* mutants, the testes were present in their normal locations and histological analysis suggested that the testes, epididymis, vas deferens and sperm production were normal. The effect of *Hoxd-10* on male fertility, therefore, is not likely to stem from abnormalities in the male reproductive system, but is likely to be operational instead. Thus, the hindlimb locomotor defects in mutant males may interfere with their ability to mount and impregnate a female.

There are no major alterations in the hindlimb musculature of *Hoxd-10* mutants since all expected distal hindlimb muscles were present in both newborn and adult mutants. Tendons derived from these muscles showed occasional abnormalities such as duplications or misrouting, and in one case there was a deletion of one of the peroneal group muscles. Preliminary observations on myosin expression indicate that the normal complement of muscle protein is produced in these muscles (Craig Neville and Nadia Rosenthal, personal communication).

Hox genes have been implicated in pattern formation of the central nervous system at the level of the hindbrain. *Hox* gene activity is required for the production and/or maintenance of rhombomeres (Carpenter et al., 1993; Mark et al., 1993) and for the production of facial motor neurons (Barrow and Capecchi, 1996; Goddard et al., 1996; Studer et al., 1996). *Hox* genes are also expressed in the developing spinal cord, where they may act as regulators of neuronal identity. Embryological studies have suggested that the segmented appearance of spinal nerves and dorsal root ganglia is generated by the surrounding paraxial mesoderm (Detweiler, 1934; Keynes and Stern, 1984;

Phelan and Hollyday, 1990). This implies that there is no intrinsic segmental organization in the spinal cord. However, there are some intrinsic features of spinal cord patterning which may result from activity of *Hox* genes or other transcriptional regulators. One feature is the position of the lateral motor columns (LMC) adjacent to limbs. While signals from the lateral plate mesoderm of the developing limb bud may establish the position of the LMCs, evidence from *limbless* chicken mutants (Lanser et al., 1986) and from limb ablation experiments (Hamburger, 1934; Hamburger, 1958; Oppenheim et al., 1978; Lamb, 1981; reviewed by Hamburger and Oppenheim, 1982) suggests that LMCs are produced even in the absence of a limb bud, but that limb buds are required for continued survival of LMC neurons. Our observations on *Hoxd-10* mutants, as well as published observations on other *Hox* gene mutants, suggest that these genes may contribute to the establishment of intrinsic patterning within the spinal cord (LeMouellic et al., 1992; Rijli et al., 1995). *Hoxd-10* mutant animals have a decrease in the spinal cord domain providing motor innervation via the sacral plexus as well as a shift in the segmental position of LMC neurons. Additionally, there is a decrease in fiber number in the tibial nerve and an occasional loss of the peroneal nerve. *Hoxa-10* mutant animals also show alterations in peripheral nerves (Rijli et al., 1995), which may reflect concomitant alterations in the spinal cord. *Hoxc-8* mutants have defects in autopod clenching which may also result from motor neuron defects at the brachial levels (LeMouellic et al., 1992).

Alterations in the peripheral nerves in *Hoxa-10* mutants are particularly interesting in light of our current observations on *Hoxd-10* mutants. Rijli et al. (1995) interpret their peripheral nerve alterations as anterior transformations of the spinal nerves emanating from segments T13 through a duplicated L5 (corresponding to wild-type T13 through L6). This suggests that a homeotic transformation of central nervous system structures (e.g., the point of origin of the spinal nerves) is occurring and that it is anterior to the transformation observed in the vertebral column. *Hoxd-10* mutants suggest similar transformations in the spinal cord and vertebral column. We observed a reduction in the number of spinal segments providing motor innervation through the sacral plexus during embryogenesis and a shift in the position of the major populations of neurons in the LMC of newborn animals. These two observations could be explained by proposing an anterior transformation in the spinal cord such that the spinal L3 segment is transformed anteriorly to L2 with no additional posterior segments undergoing transformation (Fig. 8). Thus, there would be no overall change in the number of spinal cord segments. Lateral motor column motor neuron histogenesis occurs in L1 through L6 (Lance-Jones, 1982) with the embryonic motor neurons projecting through the sacral plexus located in L3 through L6. An L3 to L2 transformation would reduce the number of motor neurons projecting through the sacral plexus. The reduction in spinal nerves passing through the sacral plexus supports this hypothesis. Additionally, part of the tibial and peroneal motor pools are derived from L3 (McHanwell and Biscoe, 1981), so the reduction in fiber number in the developing tibial nerve and occasional deletion of the peroneal nerve might reflect the deletion or respecification of those motor neurons which would normally be generated in L3.

The neuronal defects observed in *Hoxd-10* mutants are more

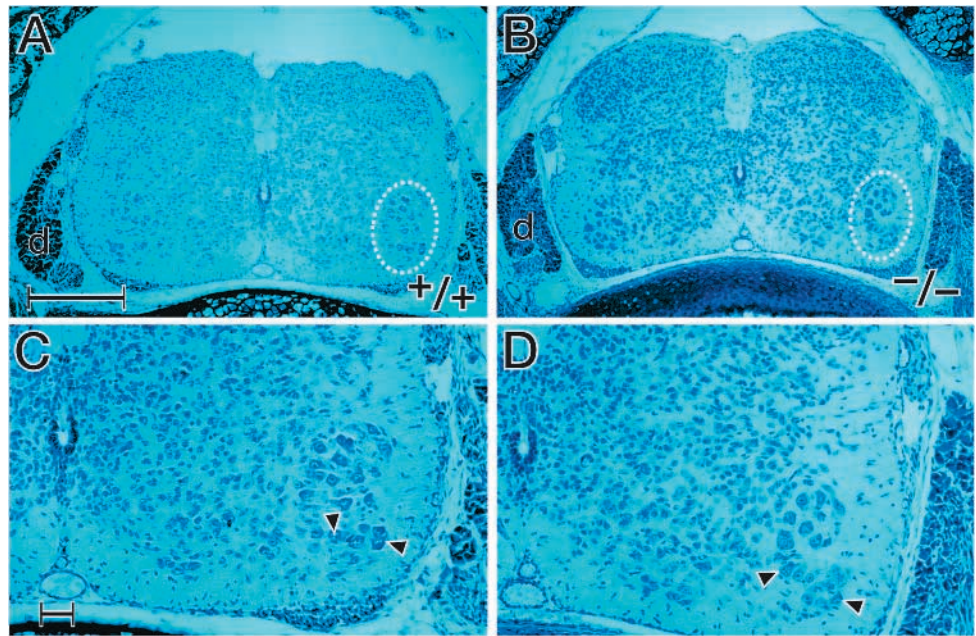


Fig. 7. Transverse sections through the spinal column of wild-type (A), and *Hoxd-10* mutant (B) newborn mice. The position of the lateral motor column is outlined. Higher magnification views of the same sections (C,D) show large motor neurons in the LMC in both animals (arrowheads). d, dorsal root ganglion. Scale bar for A and B, 100 μ m and for C and D, 20 μ m. Dorsal is up.

pronounced in embryos and newborn mice than in adults. This difference may reflect the plasticity of the nervous system. Motor neurons are, as most neurons, produced in excess and then reduced through apoptosis during refinement of the neuron-target connections. Since the *Hoxd-10* mutation appears to reduce but not eliminate the allocation of nerves to the sacral plexus, gross neuroanatomical defects are not apparent in the adult. This may reflect a rescue of cells normally destined for apoptosis or a recruitment of ectopic neurons to provide distal limb innervations. It will be of interest, however, to determine whether fine motor control in the hindfeet has been compromised in these mutants.

A possibility exists that the changes in prevertebral identity observed in *Hoxa-10* and *Hoxd-10* mutant mice influence the patterning of the nervous system in these mutant mice. This appears unlikely since in both *Hoxa-10* and *Hoxd-10* mutant homozygotes the alterations in the nervous system occur anteriorly to those observed in the vertebral column (Rijli et al., 1995; and this report). In the *Hoxd-10* mutants the spinal cord defects occur at the lumbar level and influence the generation of the lumbar LMC, while the vertebral transformations occur at the sacral level. This is consistent with Hox gene expression domains in the neural tube being maintained at levels anterior to those in the prevertebral column (Dollé and Duboule, 1989; Haack and Gruss, 1993). However, at E9 the separation of *Hoxd-10* expression in the neural tube and paraxial mesoderm is not as great (Zákány et al., 1997), allowing for possible overlap at these early time points. Unambiguous allocation of intrinsic or extrinsic specification of the spinal motor column may require the use of conditional mutations directed at selective inactivation of these genes in the neural tube or surrounding mesoderm.

The phenotypic consequences of targeted disruption of the *Hoxd-10* locus appear to be limited to inactivation of this gene alone (i.e., there do not appear to be contributions from an altered function of adjacent genes). Two observations support this idea. First, there are no apparent overlaps between the

reported mutant phenotypes of *Hoxd-9*, *Hoxd-10* and *Hoxd-11* mutant homozygotes (Davis and Capecchi, 1994; Favier et al., 1995; Favier et al., 1996). Second, no significant changes in *Hoxd-9* and *Hoxd-11* expression patterns were evident in *Hoxd-10* homozygous mutants relative to wild-type embryos.

In summary, *Hoxd-10* mutant mice show deficits in locomotion and adduction in the hindlimbs. The locomotor defects appear to be due to a malformed knee joint and a rotation of the tibia and fibula relative to the femur. However, defects are also apparent in the formation of the motor component of the nervous system in the lumbar region. The incomplete penetrance and variable expressivity suggest that other *Hox* genes, possibly *Hoxa-10* and *Hoxc-10*, contribute to the formation and organization of these nerves. This hypothesis can be tested by analysis of mice carrying multiple *Hox* gene mutations.

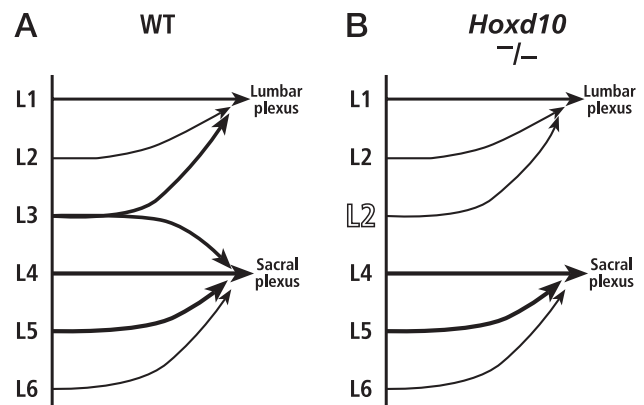


Fig. 8. Schematic representation of spinal segmental identity in wild-type (A) and *Hoxd-10* mutant (B) animals. The L3 spinal segment normally projects nerve fibers to both the lumbar and sacral plexuses. Transformation of this segment to an L2 phenotype in mutant animals (B) results in its projection only to the lumbar plexus and a deletion of the L3 projection to the sacral plexus.

Deficits in the nervous system were apparent both in terms of robustness and organization. These defects may reflect a common cause, since changes in specification of the L3 LMC would concomitantly reduce the allocation of nerves to the sacral plexus, or they may have separate causes, in which *Hox* genes would participate in decisions affecting both cell proliferation and cell specification. Irrespective of the mechanism, these studies suggest that *Hox* genes are intimately involved in the patterning of the nervous system, starting with the hindbrain and proceeding caudally along the entire axial column of the mouse.

We would like to thank C. Lenz, M. Allen, G. Peterson, E. Nakashima, M. Wagstaff and S. Barnett for excellent technical assistance and L. Oswald for preparation of the manuscript. The 2H3 neurofilament hybridoma was obtained from the Developmental Studies Hybridoma Bank under contract N01-HD-6-2915 from the NICHD.

REFERENCES

- Barrow, J. R. and Capecchi, M. R. (1996). Targeted disruption of the *hoxb-2* locus in mice interferes with expression of *hoxb-1* and *hoxb-4*. *Development* **122**, 3817-3828.
- Carpenter, E. M., Goddard, J. M., Chisaka, O., Manley, N. R. and Capecchi, M. R. (1993). Loss of *Hox-A1* (*Hox-1.6*) function results in the reorganization of the murine hindbrain. *Development* **118**, 1063-1075.
- Chen, F. and Capecchi, M. R. (1997). Targeted mutations in *Hoxa-9* and *Hoxb-9* reveal synergistic interactions. *Dev. Biol.* **181**, 186-196.
- Chisaka, O. and Capecchi, M. R. (1991). Regionally restricted developmental defects resulting from targeted disruption of the mouse homeobox gene *Hox-1.5*. *Nature* **350**, 473-479.
- Condie, B. G. and Capecchi, M. R. (1994). Mice with targeted disruptions in the paralogous genes *Hoxa-3* and *Hoxd-3* reveal synergistic interactions. *Nature* **370**, 304-307.
- Davis, A. P. and Capecchi, M. R. (1994). Axial homeosis and appendicular skeleton defects in mice with a targeted disruption of *Hoxd-11*. *Development* **120**, 2187-2198.
- Davis, A. P. and Capecchi, M. R. (1996). A mutational analysis of the 5' *HoxD* genes: dissection of genetic interactions during limb development in the mouse. *Development* **122**, 1175-1185.
- Davis, A. P., Witte, D. P., Heieh-Li, H. M., Potter, S. S. and Capecchi, M. R. (1995). Absence of radius and ulna in mice lacking *Hoxa-11* and *Hoxd-11*. *Nature* **375**, 791-795.
- Deng, C., Thomas, K. R. and Capecchi, M. R. (1993). Location of crossovers during gene targeting with insertion and replacement vectors. *Mol. Cell. Biol.* **13**, 2134-2140.
- Detweiler, S. R. (1934). An experimental study of spinal nerve segmentation in *Amblystoma* with reference to the plurisegmental contribution to the brachial plexus. *J. Exp. Zool.* **67**, 395-441.
- Dollé, P. and Duboule, D. (1989). Two gene members of the murine HOX-5 complex show regional and cell-type specific expression in developing limbs and gonads. *EMBO J.* **8**, 1507-1515.
- Dollé, P., Izpisua-Belmonte, J.-C., Falkenstein, H., Renucci, A. and Duboule, D. (1989). Coordinate expression of the murine *Hox-5* complex homeobox-containing genes during limb pattern formation. *Nature* **342**, 767-772.
- Dollé, P., Dierich, A., LeMeur, M., Schimmang, T., Schuhbauer, B., Chambon, P. and Duboule, D. (1993). Disruption of the *Hoxd-13* gene induces localized heterochrony leading to mice with neotenic limbs. *Cell* **75**, 431-441.
- Duboule, D. and Dollé, P. (1989). The structural and functional organization of the murine *Hox* gene family resembles that of *Drosophila* homeotic genes. *EMBO J.* **8**, 1497-1505.
- Duboule, D. (1991). Patterning in the vertebral limb. *Curr. Opin. Genet. Dev.* **1**, 211-216.
- Duboule, D. (1994). Temporal colinearity and the phylotypic progression: a basis for the stability of a vertebrate Bauplan and the evolution of morphologies through heterochrony. *Development* **1994 Supplement**, 135-142.
- Favier, B., LeMeur, M., Chambon, P. and Dollé, P. (1995). Axial skeleton homeosis and forelimb malformations in *Hoxd11* mutant mice. *Proc. Natl. Acad. Sci. USA* **92**, 310-314.
- Favier, B., Rijli, F. M., Fromental-Ramain, C., Fraulob, V., Chambon, P. and Dollé, P. (1996). Functional cooperation between the non-paralogous genes *Hoxa-10* and *Hoxd-11* in the developing forelimb and axial skeleton. *Development* **122**, 449-460.
- Fromental-Ramain, C., Warot, X., Lakkaraju, S., Favier, B., Haack, H., Birling, C., Dierich, A., Dollé, P. and Chambon, P. (1996a). Specific and redundant functions of the paralogous *Hoxa-9* and *Hoxd-9* genes in forelimb and axial skeleton patterning. *Development* **122**, 461-472.
- Fromental-Ramain, C., Warot, X., Messadecq, N., LeMeur, M., Dollé, P. and Chambon, P. (1996b). *Hoxa-13* and *Hoxd-13* play a crucial role in the patterning of the limb autopod. *Development* **122**, 2997-3011.
- Goddard, J. M., Rossel, M., Manley, N. R. and Capecchi, M. R. (1996). Mice with targeted disruption of *Hoxb-1* fail to form the motor nucleus of the VIIth nerve. *Development* **122**, 3217-3228.
- Graham, A., Papalopulu, N. and Krumlauf, R. (1989). The murine and *Drosophila* homeobox gene complexes have common features of organization and expression. *Cell* **57**, 367-378.
- Haack, H. and Gruss, P. (1993). The establishment of murine *Hox-1* expression domains during patterning of the limb. *Dev. Biol.* **157**, 410-422.
- Hamburger, V. (1934). The effects of wing bud extirpation on the development of the central nervous system in chick embryos. *J. Exp. Zool.* **68**, 449-494.
- Hamburger, V. (1958). Regression versus peripheral control of differentiation in motor hypoplasia. *Am. J. Anat.* **102**, 365-410.
- Hamburger, V. and Oppenheim, R. W. (1982). Naturally occurring neuronal death in vertebrates. *Neurosci. Comm.* **1**, 39-55.
- Horan, G. S. B., Kovács, E. N., Behringer, R. R. and Featherstone, M. S. (1995a). Mutations in paralogous *Hox* genes result in overlapping homeotic transformations of the axial skeleton: Evidence for unique and redundant function. *Dev. Biol.* **169**, 359-372.
- Horan, G. S. B., Ramírez-Solis, R., Featherstone, M. S., Wolgemuth, D. J., Bradley, A. and Behringer, R. R. (1995b). Compound mutants for the paralogous *Hoxa-4*, *Hoxb-4*, and *Hoxd-4* genes show more complete homeotic transformations and a dose-dependent increase in the number of vertebrae transformed. *Genes Dev.* **9**, 1667-1677.
- Izpisua-Belmonte, J.-C., Falkenstein, H., Dollé, P., Renucci, A. and Duboule, D. (1991). Muringe genes related to the *Drosophila AbdB* homeotic gene are sequentially expressed during development of the posterior part of the body. *EMBO J.* **10**, 2279-2289.
- Keynes, R. J. and Stern, C. D. (1984). Segmentation in the vertebrate nervous system. *Nature* **310**, 786-789.
- Kondo, T., Dollé, P., Zákány, J. and Duboule, D. (1996). Function of posterior *HoxD* genes in the morphogenesis of the anal sphincter. *Development* **122**, 2651-2659.
- Krumlauf, R. (1994). *Hox* genes in vertebrate development. *Cell* **78**, 191-201.
- Lamb, A. (1981). Target dependency of developing motoneurons in *Xenopus laevis*. *J. Comp. Neurol.* **203**, 157-171.
- Lance-Jones, C. (1982). Motoneuron cell death in the developing lumbar spinal cord of the mouse. *Dev. Brain Res.* **4**, 473-479.
- Lanser, M. E., Carrington, J. L. and Fallon, J. F. (1986). Survival of motoneurons in the brachial lateral motor column of *limbless* mutant chick embryos depends on the periphery. *J. Neurosci.* **6**, 2551-2557.
- LeMouellic, H., Lallemand, Y. and Brulet, P. (1992). Homeosis in the mouse induced by a null mutation in the *Hox-3.1* gene. *Cell* **69**, 251-264.
- Mansour, S. L., Thomas, K. R. and Capecchi, M. R. (1988). Disruption of the proto-oncogene *int-2* in mouse embryo-derived stem cells: a general strategy for targeting mutations to non-selectable genes. *Nature* **336**, 348-352.
- Mansour, S. L., Goddard, J. M. and Capecchi, M. R. (1993). Mice homozygous for a targeted disruption of the proto-oncogene *int-2* have developmental defects in the tail and inner ear. *Development* **117**, 13-28.
- Marieb, E. N. (1995). *Human Anatomy and Physiology*, 3rd Edition. Redwood City, CA: Benjamin/Cummings.
- Mark, M., Lufkin, T., Vonesch, J.-L., Ruberte, E., Olivo, J.-C., Dollé, P., Gorry, P., Lumsden, A. and Chambon, P. (1993). Two rhombomeres are altered in *Hoxa-1* mutant mice. *Development* **119**, 319-338.
- McHanwell, S. and Biscoe, T. J. (1981). The localization of motoneurons supplying the hindlimb muscles of the mouse. *Phil. Trans. R. Soc. Lond. B.* **293**, 477-508.
- Nagy, A., Rossant, J., Nagy, R., Abramow-Newerly, W. and Roder, J. C. (1993). Derivation of completely cell culture-derived mice from early-passage embryonic stem cell. *Proc. Natl. Acad. Sci. USA* **90**, 8424-8428.
- Oppenheim, R. W., Chu-Wang, I. and Maderdrut, J. L. (1978). Cell death of

- motoneurons in the chick embryo spinal cord. III. The differentiation of motoneurons prior to their induced degeneration following limb-bud removal. *J. Comp. Neurol.* **177**, 87-112.
- Phelan, K. A. and Hollyday, M.** (1990). Axon guidance in muscleless chick wings: the role of muscle cells in motoneuronal pathway selection and muscle nerve formation. *J. Neurosci.* **10**, 2699-2716.
- Rancourt, D. E., Tsuzuki, T. and Capecchi, M. R.** (1995). Genetic interaction between *Hoxb-5* and *Hoxb-6* is revealed by nonallelic noncomplementation. *Genes Dev.* **9**, 108-122.
- Renucci, A., Zappavigna, V., Zákány, J., Izipisúa-Belmonte, J. C., Burki, K. and Duboule, D.** (1992). Comparison of mouse and human HOX-4 complexes defines conserved sequences involved in the regulation of Hox-4.4. *EMBO J.* **11**, 1459-1468.
- Rijli, F. M., Dollé, P., Fraulon, V., LeMeur, M. and Chambon, P.** (1994). Insertion of a targeting construct in a *Hoxd-10* allele can influence the control of *Hoxd-9* expression. *Dev. Dynamics* **201**, 366-377.
- Rijli, F. M., Matyas, R., Pellegrini, M., Dierich, A., Gruss, P., Dollé, P. and Chambon, P.** (1995). Cryptorchidism and homeotic transformations of spinal nerves and vertebrae in *Hoxa-10* mutant mice. *Proc. Natl. Acad. Sci. USA* **92**, 8185-8189.
- Satokata, I., Benson, G. and Maas, R.** (1995). Sexually dimorphic sterility phenotypes in *Hoxa10*-deficient mice. *Nature* **374**, 460-463.
- Scott, M. P.** (1992). Vertebrate homeobox gene nomenclature. *Cell* **71**, 551-553.
- Small, K. M. and Potter, S. S.** (1993). Homeotic transformations and limb defects in *HoxA-11* mutant mice. *Genes Dev.* **7**, 2318-2328.
- Studer, M., Lumsden, A., Ariza-McNaughton, L., Bradley, A. and Krumlauf, R.** (1996). Altered segmental identity and abnormal migration of motor neurons in mice lacking *Hoxb-1*. *Nature* **384**, 630-634.
- Thomas, K. R. and Capecchi, M. R.** (1987). Site-directed mutagenesis by gene targeting in mouse embryo-derived stem cells. *Cell* **51**, 503-512.
- van der Hoeven, F., Zákány, J. and Duboule, D.** (1996). Gene transpositions in the *HoxD* complex reveal a hierarchy of regulatory controls. *Cell* **85**, 1025-1035.
- Zákány, J. and Duboule, D.** (1996). Synpolydactyly in mice with a targeted deficiency in the *HoxD* complex. *Nature* **384**, 69-71.
- Zákány, J., Gérard, M., Favier, B. and Duboule, D.** (1997). Deletion of a *HoxD* enhancer induces transcriptional heterochrony leading to transposition of the sacrum. *EMBO J.* **16**, 4393-4402.

(Accepted 9 September 1997)